

Organic mixed ionic-electronic conductors

Bryan D. Paulsen¹, Klas Tybrandt², Eleni Stavrinidou², Jonathan Rivnay^{1,3*}

¹ Dept. of Biomedical Engineering, Northwestern University, Evanston, IL, USA

² Laboratory of Organic Electronics, Department of Science and Technology, Linköping University, Norrköping, Sweden

³ Simpson Querrey Institute, Northwestern University, Chicago, IL, USA

*corresponding author: jrivnay@northwestern.edu

Abstract

Materials that efficiently transport and couple ionic and electronic charge are key to advancing a host of technological developments for next generation bioelectronic, optoelectronic, and energy storage devices. Here we highlight key progress in the design and study of organic mixed ionic-electronic conductors (OMIECs), a diverse family of soft synthetically tunable mixed conductors. Across applications, the same interrelated fundamental physical processes dictate OMIEC properties and determine device performance. Owing to ionic and electronic interactions and coupled transport properties, OMIECs demand special understanding beyond knowledge derived from the study of organic thin films and membranes meant to support either electronic or ionic processes only. We address seemingly conflicting views and terminology regarding charging processes in these materials, and highlight recent approaches that extend fundamental understanding and contribute to materials advancement. Further progress is predicated on multimodal and multi-scale approaches to overcome lingering barriers to OMIEC design and implementation.

Coupling between ions and electronic species is crucial for a host of applications underpinning societal needs from energy storage to health technologies. Organic materials that efficiently support both types of transport have emerged in the last decades as ideal materials for such applications owing to their processability and potential for high throughput, but more recently, for their enhanced storage and coupled transport properties. Organic mixed ionic electronic conductors (OMIECs) are soft electrical (semi-)conductors, often polymers, that readily solvate and transport ionic species. The development of OMIECs mirrors the more general development of organic π -conjugated polymers and small molecules. For many OMIECs, their ion conducting properties were inadvertent and overlooked as the focus was often purely on their electrical properties. For instance, the most ubiquitous OMIEC, poly(3,4-ethylenedioxythiophene):poly(styrenesulfonate) (PEDOT:PSS), was developed as an antistatic coating and as a hole conducting interlayer in optoelectronic devices,¹ neither of which requires ionic conductivity. Many OMIECs were the product of investigations into water soluble π -conjugated polymers to fulfill the need for materials deposition from orthogonal solvents to allow the development of multilayer, all-solution processed organic optoelectronic devices.² Irrespective of initial intent, there has been a steadily growing number of applications for π -conjugated polymers and small molecules where ion transport is crucial. The first of these applications investigated was π -conjugated polymer electrodes for batteries and super capacitors, where inducing charge within OMIECs was itself the goal.^{3,4} The field has rapidly grown to include actuators,⁵ light emitting electrochemical cells,⁶ chemical sensors,⁷ sensing and stimulating bioelectronic probes,⁸ ion pumps,⁹ and organic electrochemical transistors for sensing, circuits, and neuromorphic computing applications,^{10,11} where induced charge has enabled further functionality.

The immense diversity of OMIEC applications presents an equally extensive list of material properties targets and device figures of merit, so that these material systems might be employed to meet our ever-growing energy and health needs. This may appear to manifest itself as a collection of unrelated technological pursuits. At first pass, what does the energy density of an OMIEC-based battery have to do with the color contrast of an OMIEC-based

electrochromic display? Yet the strength of the ionic-electronic coupling that provides a high energy density also induces electronic structure changes that greatly modulate the absorption of visible light. In fact, profoundly affecting nearly all the figures of merit for OMIEC based devices are three fundamental physical processes: ionic-electronic coupling, ionic transport, and electronic transport (Table 1). For example, energy storage in OMIEC based batteries and capacitors depends on the strength of ionic-electronic coupling, whereas the available power and charging rates are often limited by the rate of ion transport. Across applications, transients are determined in large part by the efficiency of ion transport. Light emitting electrochemical cells cannot turn on until ions have migrated to form dopant gradients or junctions. The magnitude of ionic-electronic coupling determines the optical absorbance changes in electrochromics, swelling induced strain in actuators and artificial muscles, and the number of states accessible in neuromorphic devices. Ion transport and ionic-electronic coupling together determine the resistance-capacitance (RC) time constants that limit frequency bandwidth and response time of OMIEC transistors and sensors, whereas ionic-electronic coupling and electronic transport both determine the amplification capability of organic electrochemical transistors quantified as transconductance. Across applications, there is a complex interplay between these three fundamental processes.

Progress on all fronts is predicated on an advance in understanding the interrelations between ionic transport, electronic transport, and ionic-electronic coupling and their dependence on processing, synthetic structure, microstructure/morphology, and electrolyte choice. The current state of these various relations runs the gamut of well established (electronic transport dependence on ionic-electronic coupling) to incipient (ionic transport dependence on synthetic design) to essentially uninvestigated (ionic transport dependence on processing techniques). Fundamental materials structure-property relationships arising from research in any of these application-focused sub-fields presents generalizable insights useful to the field of OMIECs as a whole.

Table 1. OMIEC applications with application specific figures of merit and the associated mixed transport properties

Application	Figure of Merit	Ionic transport	Ionic-electronic coupling	Electronic transport
Batteries & Supercapacitors	Specific Energy (mWh/g), Specific Capacitance (F/g)		++	
	Specific Power (mW/g)	++	+	+
	Charging Rate (A/g, A/cm ³ , mV/s)	++		+
Light Emitting Electrochemical Cells (LEEC)	Turn-on time (s)	++		
	Luminance (cd/m ²)			+
Electrochromics	Switching Speed (s)	++		+
	Contrast Ratio (%)		++	
Organic Electrochemical Transistors (OEET)	Transconductance (mS)		++	++
	Bandwidth (Hz), response time (s)	++	++	+
Neuromorphics	Number of States		++	
	Write/read speed	++	++	
	Write Energy (J)	++	+	+
Chemical & Biological Sensors*	Sensitivity	+	++	+
	Bandwidth (Hz), response time (s)	++	+	
Actuators & Artificial Muscles	Maximum Actuator Strain (%)		++	
	Response Time (s)	++		+

+ and ++ indicate the qualitative degree to which application figures of merit depend on the various physical processes.

*The specific relationship between mixed transport processes and chemical/biological sensor metrics depend on transduction mechanism and application.

The field of OMIECs can leverage the extensive bodies of knowledge that have accumulated on electronic charge transport in conjugated organic materials, and ionic transport in

polyelectrolytes and solid polymer electrolytes. However, due to the considerable ionic-electronic coupling, ionic and electronic transport in OMIECs are not independent and must be addressed together. Those investigating OMIECs would do well to look to the work of membrane¹² and fuel cell¹³ researchers on inorganic mixed conductors. Extensive use of *operando* scattering and spectroscopy, across wide temperature ranges have provided deep insight into the fundamental physics of ionic and electronic charge transport. However, the very success of inorganic mixed conductor studies illustrates the hurdles present in OMIECs research. OMIECs are “soft” solids with weak intermolecular interactions, narrow ranges of temperature stability, and highly disordered morphology making their structure more difficult to probe with certainty. This is complicated by the fact that OMIECs are complex systems that also include mobile ions and often significant amounts of incorporated solvent which greatly modifies their structure.

Herein we review the diversity of types of OMIECs, emphasizing important differentiating characteristics. A necessary description of the fundamental mechanisms of ionic-electronic coupling and electronic and ionic charge transport is included. We highlight the important relationships between different properties and between structure and property that govern OMIEC behavior. Looking forward, we call attention to the in-situ, *operando*, and multi-modal techniques being introduced that can overcome the persistent barriers preventing a full accounting of OMIEC structure-property relationships with the hope of illuminating the path forward for OMIECs as a coherent field.

OMIEC Materials classes

OMIECs represent a subset of organic electronics that is predominated by π -conjugated polymers (CPs), but also includes radical polymers and conjugated small molecule systems. As soft materials, OMIECs are distinct from porous carbon, covalent organic frameworks, and conductive metal organic frameworks,¹⁴ which fall outside the scope of this review. In order to facilitate mixed conduction, OMIECs need either to contain or readily solvate mobile ionic species. This naturally distinguishes OMIECs into two categories, those which intrinsically

contain ionic charge (Fig. 1 I, III, and V) and those which do not (Fig. 1 II, IV, and VI). In the case of polymer-based OMIECs, this amounts to the distinction between polyelectrolytes and polymer electrolytes. Ionic charge bearing OMIECs contain a stable ionic moiety that is either accompanied by a counterbalancing ion, a stabilized electronic charge on a conjugated segment, or exists as a self-balanced zwitter ion.¹⁵ Alternatively, there exist OMIECs that themselves are not intrinsically charged, yet contain polar moieties that can solvate ions. In such non-charged OMIECs the ionic species are incorporated physically during deposition or from contact with an electrolyte. CPs lacking ion solvating or ionic functionality tend to be poor ionic conductors, especially in their electrochemically neutral state. The second useful categorization is between heterogenous (Fig. 1a&b) and homogenous OMIECs (Fig. 1c). Of particular interest is whether ionic and electronic transport occurs concurrently throughout a single material (homogeneous) or if there is segregation between regions of predominantly ion conducting material and predominantly electronic conducting material (heterogenous).

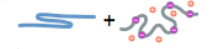
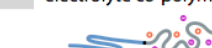
a Heterogeneous, blends, or complexed systems		b Heterogeneous block co-polymers		c Homogeneous, single component systems		
<i>Contains ions chemically linked to an insulating or conjugated component</i>	I Conjugated polymer/polyelectrolyte blends  <chem>PEDOT</chem> : <chem>PSS</chem> <i>Other examples:</i> PEDOT:Gelatin, PEDOT:DS, PANI:PSS, PPY:PSS	III Conjugated polymer/polyelectrolyte co-polymers  <chem>P3HT-b-PSS</chem> <i>Other examples:</i> PFO-b-P3PyHT	V Conjugated polyelectrolytes  <chem>PTHS</chem> <i>Other examples:</i> PEDOT-S, MPS-PPV, PBS-PFP, p(zNDI-gT2)	II Conjugated polymer/polymer electrolyte blends  <chem>MEH-PPV</chem> / <chem>PEO</chem> <i>Other examples:</i> MDMO-PPV/PEO, P3HT/PVP	IV Conjugated polymer/polymer electrolyte co-polymers  <chem>P3HT-b-PEO</chem> <i>Other examples:</i> P3EHT-b-PEO, P3DDT-b-PMMA	VI Conjugated polymer/electrolytes  <chem>p(g2T-TT)</chem> <i>Other examples:</i> p(zNDI-T2), ProDOT(OE)-DMP

Figure 1. Material classes of OMIECs. **a)** Heterogenous blends of an electronically conducting conjugated polymer with **(I)** an ionic charge bearing polyelectrolyte or **(II)** an ion solvating polymer electrolyte. These systems frequently feature impure phases and can be largely disordered on multiple length scales. **b)** Heterogenous block copolymers of an electronically conducting conjugated polymer with **(III)** an ionic charge bearing polyelectrolyte or **(IV)** an ion solvating polymer electrolyte. Such block copolymers often feature more well-defined pure phases and meso-scale order—readily synthetically tunable. **c)** Fully conjugated **(V)** ionic charge bearing polyelectrolytes and **(VI)** ion solvating polymer electrolytes. OMIEC types I-IV produce heterogenous morphologies with micro phase segregated predominately electron conducting and ion conducting domains. As shown in the sketches in the first row, in the case of blends (I & II) this occurs in a disordered fashion, or in the case of block copolymers (III & IV) it can occur in a variety of ordered structures (lamellar phase portrayed here). All-conjugated polyelectrolytes (V) and polymer electrolytes (VI) exist as a single mixed conducting phase which may contain heterogeneous composition of ordered and amorphous domains. Conceptual sketches (gray, ionic transport component; blue, electronic transport component; orange, cations; magenta, anions), example chemical structures, and selected examples are reported for type I,^{1,7,16–18} II,^{19,107,108} III,^{24,25} IV,^{20,21,23} V,^{28–31,38} and VI^{33–35} OMIECs.

Two Component OMIECs

Evaluating OMIECs based on these two categories gives rise to a taxonomy containing (at least) six types of OMIEC (Fig. 1). **I)** Heterogenous blends or complexes of an electrically conducting π -conjugated polymer and an ionically conducting polyelectrolyte are the most heavily studied class of OMIEC. Type I OMIECs include PEDOT:PSS which represents a prototypical OMIEC material.¹ Alone, PEDOT has poor solubility, so to produce dispersible suspensions it must be polymerized onto a polymer acid template, most commonly polystyrene sulfonic acid (PSS).¹ PEDOT has been templated on other polyelectrolytes,^{16,17} and other CPs have been templated on PSS^{7,18} to produce type I OMIEC materials.

Closely related are **II)** heterogenous blends of an electrically conducting π -conjugated and an ionically conducting solid polymer electrolyte. CPs incorporated in type II OMIECs are produced by traditional polymerization/synthetic techniques and require sufficient solubility so that they can be deposited with a polymer electrolyte from either the co-solvent or solvent mixtures in order to produce phase separated bicontinuous microstructures.¹⁹ Both I and II represent composites of predominately electronic and ionic conducting materials that phase separate into mostly ionic and electronic conducting phases.

Block OMIECs

Whereas I and II represent composites of two discrete molecular components, type III and IV materials are based on single macromolecules containing a distinct ionic and electronic conducting segments (figure 1b). These block macromolecular OMIECs include **III)** those which

contain a distinct fixed ionic charge bearing segment covalently tethered to a π -conjugated segment and **IV**) those which contain a distinct polar ion solvating segment covalently tethered to a π -conjugated segment. **III** and **IV** include block copolymer materials where both ionic and electronic conducting segments consist of a block of repeating sub units,^{20,21} and liquid crystalline materials²² where one or both of the segments is a single non-repeating structure. Thermodynamics drives the phase separation of the segments on length scales determined by the segment lengths.^{22,23} By tuning relative segment/block size and processing conditions, a wide array of defined structures are achievable including spherical, cylindrical, lamellar, and gyroid phases.²⁰ Given mesoscale morphological disorder, such structures (aside from spherical) should provide extended, interconnected domains for separate ionic and electronic transport. Type **III** OMIECs block copolymers with both non-conjugated²⁴ and conjugated²⁵ polyelectrolyte blocks have been demonstrated.

Single Component OMIECs

Finally, there are homogenous OMIECs (figure 1c) where there is no microphase separation between ion conducting and π -conjugated components. Type **V** and **VI** OMIECs are charged (often pendant ion sidechains) or polar (often ether oxygens incorporated into the repeat units or side chains) respectively. The distribution of ion solvating moieties along their entire molecular structure produces a single mixed conducting phase. These single-component systems share the most in common with traditional CPs, though with added functionality that improves ion miscibility even in the absence of solvent swelling. Examples of type **V** and **VI** OMIECs tend to be homopolymers, and alternating²⁶ or statistical copolymers. Type **V** sulfonate bearing poly alkylthiophenes^{27,28} and poly ethylenedioxothiophenes²⁹ have been investigated, amongst others.^{30,31} Although conjugated polymer electrolytes (**VI**) represent a recent addition to the OMIECs arena,³² they have rapidly demonstrated both hole (p-type) and electron (n-type) transport using proven backbone motifs with oligo ethylene glycol side chains.³³⁻³⁵ Conjugated small-molecule mixed conductors, such as ionic transition metal complexes³⁶ and radical polymers³⁷ both tend to present homogeneous systems akin to type **V** and **VI** respectively.

The wide area of OMIEC materials types reflects the wide array of target applications. The application-specific preference of one OMIEC over another arises from practicalities of processability, material scalability, stability, compatibility with other materials or electrolytes, or simply from the importance of one optoelectronic process far surpassing that of others. Type I OMIECs, in particular PEDOT:PSS, have been investigated broadly in electrochromic devices, supercapacitors, chemical/biological sensors, neuromorphic devices, and organic electrochemical transistors (OECTs). Type II blends and type V conjugated polyelectrolytes have been employed in light emitting electrochemical cells.¹⁹ Conjugated polyelectrolytes (III & V) have found extensive application as interlayers in optoelectronic devices and in fluorescent biosensing,³¹ and type V polyelectrolytes have been applied in electrochromic, chemical sensor, transistor, and energy storage devices.^{28,30,38} Thus far, development of conjugated block copolymers (IV) and radical polymers (VI) have focused on battery applications.^{37,39,40} Conjugated type VI OMIECs have applications in transistor and biological sensing devices.¹⁰

Even as a narrow subset of organic electronic materials, OMIECs still present a diversity of materials combinations and morphologies, accessible through a broad range of synthetic and processing techniques. These OMIEC types are certainly not absolute nor exhaustive, with some OMIEC systems blurring the lines of this classification, yet they delineate key differences in the routes taken to produce efficient mixed conduction in organic systems through materials choice, molecular design, and morphology.

Processes in OMIECs

As mentioned above, ionic and electronic transport can occur simultaneously in a homogenous OMIEC or can be segregated between solid-electrolyte rich and conjugated material rich micro-phase separated regions, respectively. Similarly, ionic-electronic coupling can occur homogeneously throughout an OMIEC, at the interface between phase separated regions, or as a more complex hierarchical intermediate case. These processes occur throughout the bulk, amounting to volumetric properties when considered from the macroscopic device level.

Whereas many electrochemical and semiconductor systems and devices depend on two dimensional materials interfaces, OMIECs present a three-dimensional volumetric interface at which ionic-electronic interactions occur.

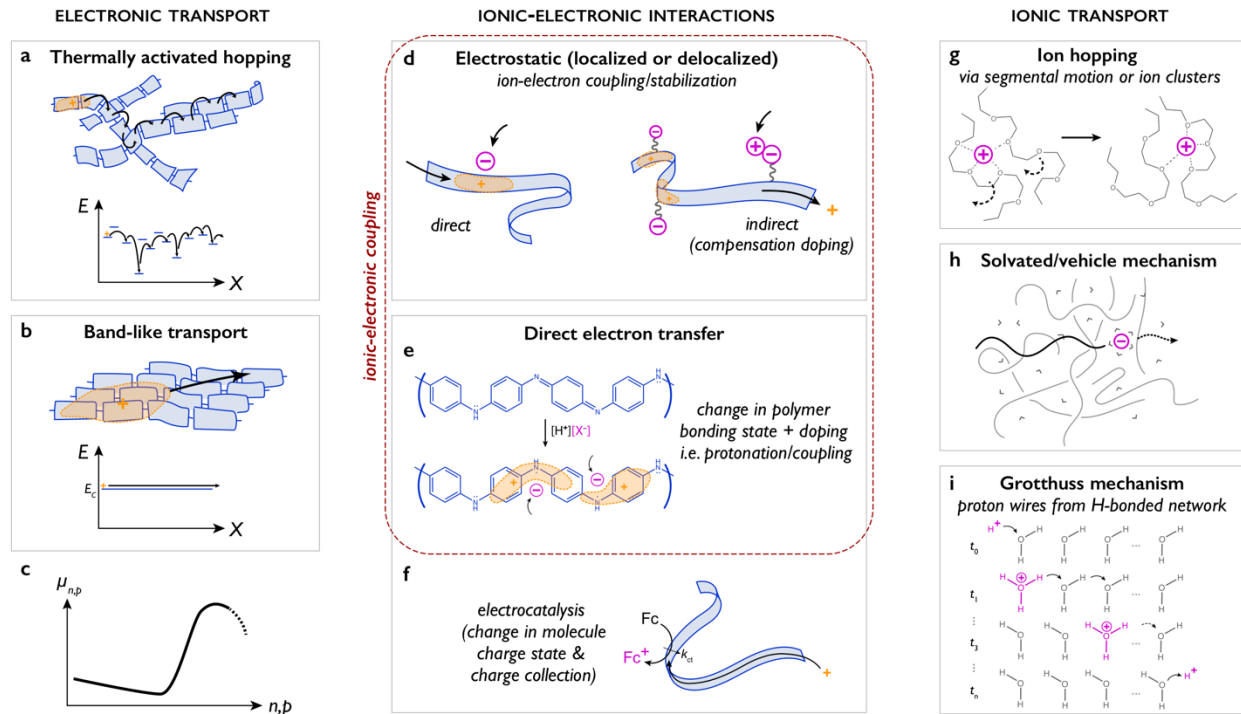


Figure 2. | Processes in OMIECs. **a-c:** the left column shows electronic charge transport mechanisms: molecular cartoon and energy schematic representing thermally activated hopping transport of a relatively localized electronic charge carrier (**a**) and band-like transport of a relatively delocalized electronic charge carrier (**b**). The functional dependence of mobility on charge carrier density (**c**) shows an initial decrease due to increased charge trapping, a steep increase of thermally activated transport, a plateau of weakly activated transport, and finally a decrease due to disorder driven localization. **d-f:** in the middle column, ionic-electronic interactions including charge coupling/stabilization through electrostatic interactions (**d**) and direct charge transfer with (**e**) and without (**f**) charge stabilization. The latter case, electrocatalysis, is not an example of ionic-electronic coupling in view of the absence of charge stabilization in the OMIEC itself. **g-i:** ionic charge transport mechanisms are reported in the right column: segmental motion assisted ion hopping (**g**), solvated ion vehicle transport (**h**), and Grotthuss mechanism of proton hopping (**i**). Elect ionic charges are shown in orange, ionic species in magenta. Polymers supporting electronic species are shown in blue.

Ionic-Electronic Interactions

How best to describe the ionic-electronic coupling in OMIECs (Fig. 2, middle column) remains somewhat controversial (see Box 1). Despite scientific disagreement, nature still demands that charge balance must be rigorously maintained, and OMIECs are no exception. For there to be a presence of electronic charge in an OMIEC requires the presence of a stabilizing excess ionic charge (net ionic charge) of the opposite sign. The counterbalancing of excess ionic charge with

electronic charge is commonly referred to as doping, as it results in increased electrical conductivity in the OMIEC. In the case of type II, IV, and VI OMIECs this stabilizing doping is achieved by the presence of mobile ions (Fig. 2d), and removal of these ions results in de-doping. In type I, III, and V OMIECs, stabilizing charge is fixed in the OMIEC, thus they can be inherently doped. Since these dopant ions cannot be removed, de-doping can occur via the incorporation of oppositely charged mobile ions that compensate the fixed ionic charge present in the OMIEC. There are some OMIECs where ionic-electronic coupling occurs through direct charge transfer, such as the protonation of polyaniline which leads to the stabilization of electronic charge (Fig. 2e). Likewise, OMIECs can serve as electrocatalytic interfaces for other redox species (Fig. 2f).⁴¹⁻⁴³ In such case, direct charge transfer occurs without the further stabilization of electronic charge in the OMIEC, and thus does not represent ionic-electronic coupling.

In the absence of an externally applied potential there is some preferred equilibrium concentration of electronic charge and counterbalancing excess ionic charge which depends on the energetic position of the OMIECs molecular orbitals. If the highest occupied molecular orbital (HOMO) of the OMIEC is sufficiently shallow, then the presence of positive electronic charge in the form of a hole on the OMIEC stabilized by an excess anion is energetically favorable, termed p-type doping. Conversely, if the lowest occupied molecular orbital (LUMO) is sufficiently deep, a cation-stabilized negative electronic charge is energetically favorable, termed n-type doping. If the HOMO is deep and LUMO shallow, then ionic-electronic charge coupling and stabilization is energetically unfavorable, and the OMIEC remains undoped with minimal electrical conductivity. As with organic electronic materials in general, p-type OMIECs are far more common than n-type. However, in LEEC applications both cationic and anionic doping are necessary for the injection and transport of electrons and holes which can recombine leading to light emission.

The amount of coupling between electronic charge and excess ionic charge (degree of doping) in OMIECs can be modulated with an applied bias when coupled through an electrolyte. This

manifests as a potential dependent capacitance (C), which is the strength of this ionic-electronic coupling characterized as the charge induced per unit voltage per volume or mass of the OMIEC. Homogenous single phase OMIECs (type V and VI) display larger magnitudes of ionic-electronic coupling and larger values of volumetric capacitances than biphasic OMIECs (type I-IV).⁴⁴ This potential-dependent coupling is the fundamental mechanism of charge storage in OMIEC based supercapacitors and batteries, and of transduction between ionic and electronic signals in OMIEC-based sensing and stimulating probes. This coupling can also lead to the filling or emptying of electronic states allowing for the reversible bleaching of optical transitions needed in electrochromic devices. Further, the modulation of the degree of doping naturally modulates the electrical conductivity of the OMIEC and is leveraged in a variety of OMIEC-based OECTs and neuromorphic devices.

Electronic Transport

Many OMIECs, as a subset of π -conjugated organic electronic materials, are governed by van der Waals interactions, often containing a significant degree of structural disorder.⁴⁵ Their high degree of π -conjugation results in weakly bound electrons that can move along a constituent molecule through delocalized π -orbitals, and between molecules where there is sufficient π - π overlap. Disorder limits the degree of delocalization and overlap leading to charge transport proceeding as series of thermally activated hops between states that lie within a statistically likely range of distance and energy (Fig. 2a), which can be described with a variety of models.^{46,47} Without doping, the electronic charge carrier density and the density of accessible hopping states is low, resulting in low electronic charge carrier mobility and low electrical conductivity.

However, in OMIECs doping is present due to ionic-electronic coupling. In application-relevant conditions, dopant concentrations and electronic charge carrier density can range over many orders of magnitude, with electronic carrier mobility depending on carrier density in a non-monotonic fashion (Fig. 2c). At very low concentrations the dopant ions act as Coulombic traps for electronic charge carriers.⁴⁸ With increasing doping levels the activation energy of charge

hopping decreases and carrier mobility increases, with some OMIECs displaying diffuse band-like charge transport (Fig. 2b).⁴⁹ At extreme doping levels, increased disorder drives carrier localization which results in a plateau or even decrease in electronic charge carrier mobility.^{49,50}

Non-conjugated radical polymers also present a thermally activated mechanism of charge transfer between pendant radical sites, though with a significant dependence on the local self-diffusion of polymer chain to bring radical sites close enough for efficient charge transfer.⁵¹ This manifests as a hopping transport of electronic carriers (Fig. 2a) that is assisted via segmental motion (described below; Fig. 2g). Also in this case disorder plays a role, producing local variations in the molecular orbital energy levels and spreading orbitals in a density of radical states.⁵² This transport mechanism results in macroscopic electrical conductivities of order 10^{-5} S cm⁻¹ (compared to 1-1000 S cm⁻¹ typical of PEDOT:PSS). However, recent work has shown that electrical conductivity in submicron domains can be as high as 10^{-2} S cm⁻¹.⁵³

Ionic Transport

What sets OMIECs apart from other π -conjugated organic semiconductors is their ability to conduct ionic currents (by a number of mechanisms, shown in Fig. 2, right column) in addition to electronic currents. The negatively charged anions and positively charged cations can be thought analogous to electrons and holes. However, ionic transport can be more complex: ions can be present in multiple species, ions can be multi-valent, and form pairs and larger clusters; moreover, they are sensitive to solvent and solvation. Ionic transport, quantified as an ionic conductivity (σ_{ionic}) represents the sum of the ion conductivities for each mobile ionic species, i , which is the sum of the products of the ion charge (z_i), number density (n_i), elementary charge (e), and mobility (μ_i):

$$\sigma_{ionic} = \sum_i n_i |z_i| e \mu_i$$

Ion mobilities and diffusivities (D) are interconvertible via the Einstein relation.

$$D = \frac{\mu k_B T}{e}$$

Where k_B is Boltzmann's constant and T is temperature.

In the case of dry OMIECs, ion transport is unipolar for types I, III, and V as one of the ionic charged species is fixed on a polyelectrolyte, whereas both anions and cations are mobile in types II, IV, and VI. For OMIECs in contact with an electrolyte, swelling occurs allowing the infiltration of excess ions from the electrolyte, thus both mobile anions and cations may contribute to ion transport.

In dry and minimally hydrated films, ion motion occurs through ion hopping coupled with the segmental motion of the OMIEC side chains or backbone. This segmental motion assisted transport can be improved with the incorporation of ion-coordinating moieties (Fig. 2g). Dry type V polyelectrolytes and type II blends have ion mobilities of order 10^{-10} and $10^{-9} \text{ cm}^2 \text{ V}^{-1} \text{ s}^{-1}$, respectively.^{54,55} OMIECs are especially sensitive to moisture content, with type V conjugated polyelectrolyte ion mobility increasing nearly four order of magnitude when increasing water content from 0.2% to 4% ($\mu_{\text{ion}} \sim 10^{-11} \text{ cm}^2 \text{ V}^{-1} \text{ s}^{-1}$ to $10^{-7} \text{ cm}^2 \text{ V}^{-1} \text{ s}^{-1}$).⁵⁶

Contact with solvent or liquid electrolyte swells OMIECs, and ion transport proceeds more rapidly through solvated ion vehicle transport (Fig. 2h). Electrolyte-swollen type I OMIEC PEDOT:PSS displays solvated cation mobilities roughly equivalent to the electrophoretic mobility of similar ions in water ($\mu_{\text{ion}} \sim 10^{-3} \text{ cm}^2 \text{ V}^{-1} \text{ s}^{-1}$ for monatomic ions).⁵⁷ In water swollen OMIEC systems, proton conduction can occur even more rapidly via the Grotthuss mechanism (Fig. 2i) of proton hopping between hydronium and water molecules in a hydrogen bonded system ($\mu_{\text{H}^+} \sim 5 \times 10^{-3} \text{ cm}^2 \text{ V}^{-1} \text{ s}^{-1}$).⁵⁸ The relationship between ionic transport and ionic-electronic coupling is not so straightforward as it is for electronic charge transport. Contact with an external electrolyte can result in OMIEC infiltration with a significant population of charge-balanced ions independent of ionic-electronic coupling.

The profound effects of ionic-electronic coupling, hydration, and electrolyte swelling complicate direct comparisons between OMIECs and inorganic mixed conductors. Inorganic mixed conductors developed for solid oxide fuel cell and hydrogen separation membranes have

high ionic and electronic conductivities, though at elevated temperatures ($>200\text{ C}$).¹³ Near room temperature, transport in inorganic and organic mixed conductors is more readily comparable. In the well-developed field of Li battery materials, ion mobility in cathode materials can approach $10^{-3}\text{ cm}^2\text{ V}^{-1}\text{ s}^{-1}$, though electrical conductivity only reaches 10^{-4} S cm^{-1} necessitating the use of conductive binders.⁵⁹

Directionality and dimensionality

The directionality and dimensionality of ion transport, electronic transport, and ionic-coupling in OMIECs depends on the application specific device geometry. As OMIECs are often employed as thin films, this results in transport occurring across drastically different length scales (nm to mm) depending on the application. OMIEC-coated electrodes used for cyclic voltammetry and impedance experiments involve parallel ionic and electronic transport through the generally tens or hundreds of nm thick films (Fig. 3a). This geometry approximates well the OMIEC active layers in sensing/stimulation, energy storage, and electrochromic devices (Fig. 3b). In these cases, at steady state, ionic-electronic coupling is generally thought to occur uniformly throughout the film.¹⁰

In light emitting electrochemical cells (Fig. 3c,d), ionic and electronic transport also occurs in the parallel, though over different length scales depending if the cell is vertical ($\sim 100\text{ nm}$) or planar ($\sim 10\text{ }\mu\text{m}$). However, ionic-electronic coupling at steady-state is non-uniform in response to the electric fields present under operating conditions. Moving front geometries (Fig. 3e) allow the spatial separation of ionic and electronic transport, with ionic-electronic coupling only occurring in the region of OMIEC infiltrated by ions. Transistor (Fig. 3f) and neuromorphic applications¹¹ (Fig. 3g) present cases of orthogonal mixed conduction, with the dominant ion transport occurring vertically into the film while electronic transport occurs laterally between electrodes through the OMIEC film. The distribution of volumetric ionic-electronic coupling depends on the applied potentials and timescales dictated by operating conditions.

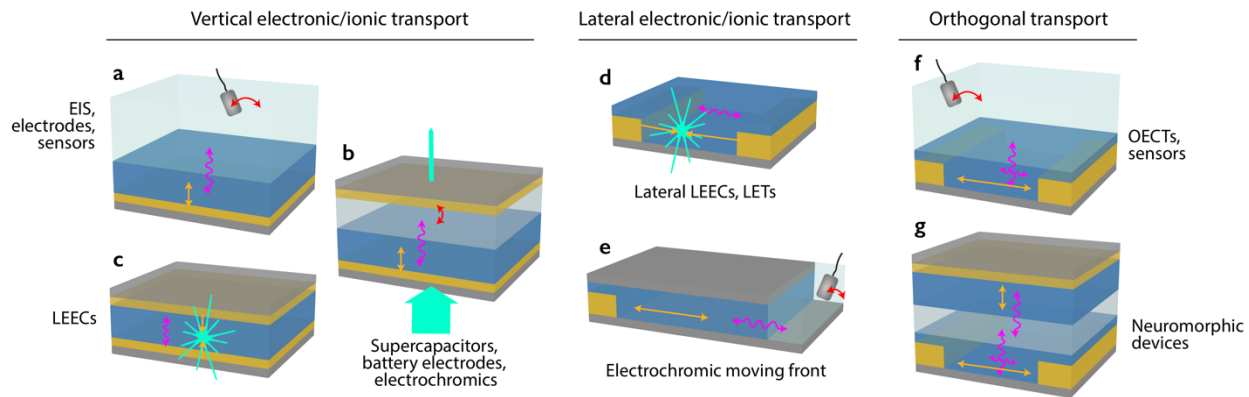
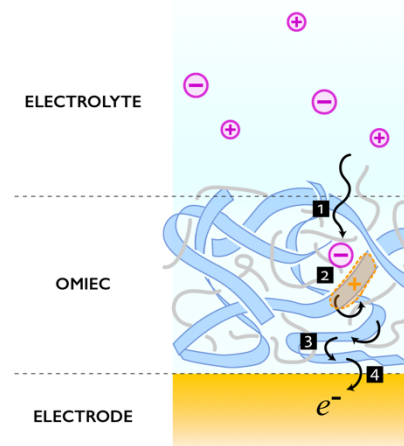


Figure 3. Typical configurations of OMIEC-based devices. The geometries are generally grouped into those that show vertical (out of film plane) ionic drift/diffusion and electronic transport (**a-c**), those that show lateral (in plane) ionic/electronic transport (**d,e**), and those with ions and electrons transported in orthogonal directions within one film or within one device (**f,g**). Devices preferentially follow one of these configurations depending on their applications: **a**, devices for electrochemical impedance spectroscopy (EIS), electrodes, sensors; **b**, supercapacitors, battery electrodes, electrochromics; **c**, light emitting electrochemical cells (LEECs); **d**, lateral LEECs, light-emitting transistors; **e**, devices for electrochromic moving front experiments; **f**, OECTs, sensors; **g**, neuromorphic devices¹¹. Electronic injection/transport is denoted by orange arrows, ionic injection/transport is denoted by magenta wavy arrows. Red arrows indicate charge balancing processes occurring at the gate or counter electrodes. Green/cyan denotes light emission or transmission in opto-electronic devices.

Box I: Charging in OMIECs: electrostatic *and* faradaic?

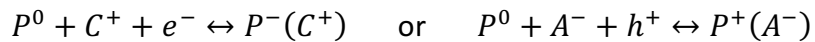
In the field there persists disagreements and confusion on how best to describe charging (ionic-electronic coupling) phenomena in OMIECs, which present a complex case (Box Figure) of a disordered, weakly interacting, low dielectric constant, molecular system infiltrated by an electrolyte. Electronic charge can be injected/collected at the electrode/OMIEC interface, transported through the π -conjugated system; and most often is electrostatically stabilized by a dopant ion supplied from the electrolyte.



Box Figure 1. Charging in OMIECs. An OMIEC in contact with a metal electrode and an electrolyte, highlighting [1] dopant ion injection and transport, [2] electronic carrier (hole) stabilization by a dopant ion (anion), [3]

electronic carrier hopping, and [4] charge transfer between the metal electrode and the OMIEC. Note: numbering does not indicate the order of the processes.

Confusing the interpretation of OMIEC behavior is the inconsistent (and seemingly contradictory) description of OMIEC charging as alternatively *faradaic*, *capacitive* (electrostatic), or *pseudocapacitive*. Faradaic charging of OMIECs implies a current corresponding to the oxidation/reduction of some chemical substance, that follows Faraday's law relating moles of product to coulombs of charge through Faraday's constant, where oxidation/reduction is the complete, net removal/addition of one or more electrons from/to a molecular entity.¹⁰⁹ There do exist cases of CPs and OMIECs that undergo archetypal integer electron redox reactions.^{38,70} Cyclic voltammograms of thin films of these materials display discrete charging waves reflecting integer electron processes localized to single polymer repeat units (P), via stabilization with a cation (C) or anion (A) supplied from the electrolyte. This yields a redox reaction description of OMIEC charging of:



The "molecular entity" being reduced is clearly definable as the polymer repeat unit, and the chemical equilibrium between neutral and reduced repeat units follows a rationalizable reaction coordinate. Electronic charge transport proceeds through mixed valance transport, with narrow conductance peaks centered around the electrochemical potential where half the population has undergone a redox process.⁷⁰ The ideality of such a system is due the charge localization to a single polymer repeat unit.

However, such exceptions only prove the more common rule that most CPs generally do not undergo neat redox processes of clearly defined "molecular entities". More often, charge is delocalized and distributed fractionally over a non-constant number of repeat units, and this degree of delocalization depends greatly on the intermolecular ordering. For example, in polyalkylthiophene-based materials the neutral ring stretch modes are completely quenched at a doping concentration of only 0.05 charges per thiophene repeat unit,⁷¹ yet peak conductivity does not occur until 0.15 charges per repeat unit, and charging can continue up to levels of ~0.5 charges per repeat units.⁵⁰ This is to say that from a redox reaction

perspective, while the neutral reactant is completely consumed, the “reaction” of charging continues. This cannot be rationalized as an equilibrium between a neutral and integer charged species, but instead is a continually evolving equilibrium between incrementally differing degrees of fractional charge. This makes it exceedingly difficult to define reactants, products, and integer electron processes in OMIECs, such that referring to these systems as undergoing faradaic redox processes gives little insight into the actual phenomena.

Further complicating matters is the common perception that faradaic and electrostatic are mutually exclusive, with reports arguing that charging is either a faradaic redox process or a non-faradaic electrostatic process. This is a false dichotomy. While the example of doping via protonation is faradaic and non-electrostatic (Figure 2e), most ionic-electronic charge coupling phenomena in OMIECs are faradaic *and* electrostatic. Even in the case of ideal redox polymers (described above), the interaction between electronic charge on the reduced repeat unit and the stabilizing cation is electrostatic. Charge transfer occurs between the OMIEC and the contacting metal electrode, *not* between repeat units and the stabilizing (dopant) cations. Understanding OMIEC charging to be faradaic does not preclude electrostatic charge interactions.

Finally, OMIEC charging is often referred to as pseudocapacitive, displaying additional capacitance beyond what is expected for an electric double layer. Does the pseudocapacitive nature of OMIEC charging arise out of the perceived redox nature of polymer itself, the intercalation of dopant ions within the OMIEC, the possible desolvation of said dopant ions, and/or some ion absorption effect? Considering OMIECs are pseudocapacitive because they are assumed to undergo faradaic redox processes clarifies little. Without specifying the manner in which OMIECs are pseudocapacitive (which is likely very complicated), the term imparts little insight into the physical phenomena. Instead of relying on unnecessarily vague terms, accurate descriptions of charging must better connect to the physical phenomena. Some more insightful routes include considering the distribution of electronic states,⁵² the effects of intermolecular interactions and disorder,⁸⁰ the energy-level description of OMIEC

devices,¹¹⁰ and the complicated electrostatic and chemical potential landscapes of biphasic OMIECs.⁸¹ How best to describe OMIEC charging remains controversial, but the controversy is far more interesting than electrostatic versus faradaic.

Quantifying Interrelated OMIEC Properties

As described above, OMIECs present a complicated case of multiple highly interacting charged species. Thus, accurately isolating and quantifying ionic and electronic transport is a challenging endeavor. Electrochemical impedance spectroscopy (EIS) presents a possible route to simultaneously deconvolute and characterize ionic and electronic transport and quantify ionic-electronic coupling (Fig. 3a). Used widely in electrochemistry and in the development of inorganic mixed conductors,⁶⁰ EIS is a method of current-voltage small signal analysis to measure the frequency-dependent complex impedance of an OMIEC film, with the real and imaginary components providing information on the OMIEC's ability to pass and store charge, respectively.⁶¹ EIS has been used to extract mobilities and conductivities of electronic⁶² and ionic transport,^{63,64} and ionic-electronic coupling in the form of volumetric capacitance or electrochemical density of states.⁶⁵

To extract these parameters, the complex impedance measured by EIS is rationalized with the help of an equivalent circuit. Although some systems are adequately modeled with simple circuits, OMIECs generally present much more complicated impedance spectra requiring the use of transmission line models borrowed from porous electrode models,⁶⁶ Warburg diffusion elements,⁶⁷ or constant phase elements.⁶¹ Unfortunately, as the complexity of the equivalent circuitry grows, the connection between circuit elements and physical phenomena can grow tenuous, and multiple equivalent circuits assuming conflicting physical phenomena can produce adequate fits. Nevertheless, EIS provides the most common route to characterize the magnitude of ionic-electronic coupling in the form of a voltage and frequency dependent capacitance. Given the absence of significant side reactions or electrolyte breakdown or major

hysteresis, cyclic voltammetry can be integrated to provide a capacitance estimate equivalent to the EIS derived capacitance in the low frequency limit.

OECTs can be used as test beds to isolate the ionic-electronic coupling dependent electronic charge transport behavior of the OMIEC they are made of. OECTs are analogous to traditional three terminal field effect transistors, with an OMIEC thin film as the semiconductor channel, and the gate dielectric replaced with an ion conducting electrolyte (Figure 3f). The OECT geometry allows for the dimensional decoupling of the electronic currents travelling laterally through the OMIEC channel from the ionic charging currents of the gate-channel circuit. The gate voltage tunes the three-dimensional ionic-electronic coupling (doping) through the OMIEC channel, thus modulating the electrical conductivity.⁶⁸ Electronic charge carrier mobilities can be extracted by estimating the electronic charge carrier density from EIS-determined volumetric capacitance or integrating the gate charging currents.⁵⁰ Alternatively, time or frequency-domain gate current analysis allow for the extraction of electronic carrier transit times and thus electronic carrier mobility.^{68,69} The nature of these dopant-induced charge carriers is often probed with UV-vis,⁷⁰ infrared,⁷¹ or electron resonance⁴⁸ spectroelectrochemical techniques.

Isolating the ionic charge transport presents its own set of challenges. Scanning probe techniques have been employed to monitor ion transport in dry OMIEC films.⁵⁴ Combined muon spin relaxation and electron paramagnetic resonance spectroscopies has been employed to deconvolute proton transport in melanin.⁷² Monitoring of the progression of moving redox fronts in OMIECs, first developed for CPs, has been an alternative, direct experimental approach to isolate and quantify ionic transport.⁷³ By contacting an OMIEC film with a spatially separated electrode and electrolyte, upon the application of a bias, a moving redox front is formed in the OMIEC between the electrode and the electrolyte (Fig. 3e). The electrode is a source/sink for electronic charge for the OMIEC film, thus electronic transport occurs between the electrode and the moving front. Conversely, the electrolyte can only supply ionic charge, thus between the electrolyte and the moving front only ionic transport occurs. The velocity of

the moving front is determined by the rate-limiting charge transport, often the ionic transport. Due to OMIECs electrochromic nature, the motion of the moving front can be tracked with photographic and spectroscopic techniques.^{57,74-76} Applying EIS techniques in a moving-front geometry can relate ion transport and ionic-electronic coupling,⁷⁷ which for the most part is an unexplored property interrelation.

The above methods generally provide empirical current-voltage relationships to describe mixed transport and ionic-electronic coupling. These inherently represent macroscopic summations of microscopic processes, and rigorous modelling is needed to properly discern their physical mechanisms. Early modelling employed classical electrochemical diffusion (Cottrell) and kinetic (Butler-Volmer) models, which with the inclusion of a phenomenological capacitance term allowed the qualitative capture of the main features of OMIEC charging behavior,⁷⁸ and were further refined by considering the drift-diffusion of ions within the OMIEC.⁷⁹ While these models only focused on ionic transport, the growth of interest in OECTs led to the development of models that reproduced electronic charge transport and charging transient behavior by considering the field-dependent drift of both ionic and electronic species.⁶⁸ Such OECT models were further refined by considering the charge-dependent electronic mobility and a disorder-broadened density of states.⁸⁰ These works have culminated in the development of models that quantitatively reproduce both charging and transport behavior, by accounting for the drift-diffusion of both ionic and electronic species, and in the prototypical case PEDOT:PSS, considering the effect of the capacitance between the PEDOT and PSS phases on the Fermi level of the PEDOT.⁸¹

Unravelling structure-property relations

Ultimately the properties of ionic-electronic coupling, ionic transport, and electronic transport in OMIECs are determined by the complex interplay between synthetic design, electrolyte choice, processing, and microstructure which all serve to determine application specific device performance (Figure 4). The interrelated ionic/electronic properties are *directly* influenced by synthetic design and electrolyte choice. Additionally, synthetic design and electrolyte choice

along with processing *indirectly* determine transport/coupling properties through their impact on OMIEC microstructure, ultimately affecting application-specific device performance.

Both the dependence of structure on synthetic design and processing, and the relationship between electronic transport and ionic-electronic coupling have been extensively studied in CPs; yet the collective understanding of other structure-property and property-property relationships is not as mature. Especially rare are reports elucidating the effects of electrolyte choice and the interrelations between ionic transport and electronic transport, and ionic transport and ionic-electronic coupling. As highlighted in Figure 4, this leads to clear road blocks to the overall goal of improved performance of OMIEC devices.

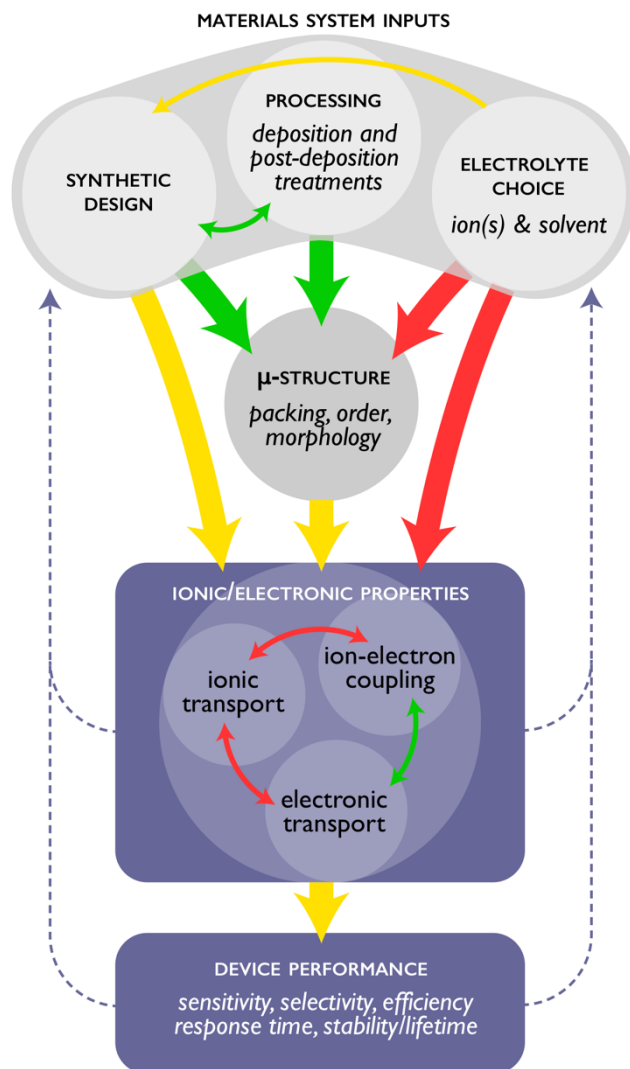


Figure 4. Understanding interrelations in OMIECs. Synthetic design, processing and electrolyte choice impact the microstructure of OMIECs and ultimately determine the ionic and electronic properties of these materials and their performance in device applications. Arrow colours indicate the current degree of understanding of these interrelations: well-developed areas of study in green, areas of growing interest in yellow, areas critically understudied in red. Robust interrelations are necessary for informed feedback to direct OMIEC design (dotted purple lines).

Synthetic Design and Electrolyte Choice

Being organic materials, OMIECs benefit from vast synthetic tunability. The synthetic design rules from CPs, polyelectrolytes, and polymer electrolytes can be applied to the synthesis of OMIECs.^{82,83} Efficient electronic transport in CPs depends on proper choice of repeat units and side chains to drive molecular ordering and chain planarity, and adequate molecular weight for the interconnectivity of ordered domains leading to a percolative path for efficient macroscopic electrical conductivity.⁴⁵ Achieving ionic-electronic coupling at accessible potentials requires the engineering of HOMO/LUMO levels with electron rich and deficient moieties.⁸² Ion miscibility depends on the polar or ionic repeat units of the polymer electrolyte or polyelectrolyte, respectively. The molecular weight and chain architecture must be selected to promote segmental motion and avoid crystallinity that is detrimental to most ion transport.⁸⁴ In two-component and block OMIECs (type I-IV) where the electronic transport and ionic transport occur largely in separate phases, the synthetic routes to efficient ionic and electronic transport can be independently applied in designing the respective components and blocks.

The synthetic design of single phase OMIECs (type V and VI) that efficiently transport both ionic and electronic charge is more complicated. The synthetic routes for high degrees of order that benefit electronic transport are at odds with the synthetic routes promoting segmental motion and swellability that benefit ionic transport. Despite the compromise between ionic and electronic transport, type V and VI OMIECs benefit from a marked increase in ionic-electronic coupling (capacitance) over two-component and block co-polymer systems.⁴⁴ Currently rational synthetic design of OMIECs is still in its infancy, and it is not clear yet whether the synthetic paths to highly ionically and electronically conducting OMIECs are not definitively incompatible.

In addition to synthetic design, electrolyte choice is also important in determining OMIEC properties. Ionic conductivity is generally inversely proportional to the hydrated ion radius,⁵⁷ thus it is affected by the choice and concentration of ions. Ion choice can also affect electronic transport as in both polythiophene and PEDOT-based materials the electronic charge carrier mobility ranges over three orders of magnitude depending on the nature of the ion dopant (be it mobile ions, side chain tethered ions, or polyelectrolyte ions). Some fluorinated ions are more susceptible to hydrolyzation, producing acid species which can oxidize an OMIEC, modifying its electronic transport properties and ionic-electronic coupling.⁸⁵

The choice of electrolyte inherently affects the OMIEC composition. In dry applications such as LEECs, the OMIEC average composition is determined by the materials deposited. However, during device operation, significant ion motion occurs in response to applied fields. Scanning probe techniques have revealed that anions and cations accumulate near opposite electrode interfaces producing p-i-n junctions in type **VI** small-molecule OMIEC films,⁸⁶ and redistribute creating expansive cation-rich and anion-rich regions producing p-n junctions in type **IV** CP/polymer electrolyte blends.⁸⁷ Spatially resolved Raman spectroscopic studies of OECTs have shown that electronic and ionic charge concentrations vary considerably across device-pertinent length scales under operating conditions.^{88,89}

The composition of OMIECs in electrolyte-immersed applications is far more complicated, as many OMIECs are known to swell upon exposure to solvents and electrolytes (Fig. 5a-d). The ion and solvent infiltration depend on the electrochemical potential and the concentration of the interfacing electrolyte. Volumetric changes of OMIEC thin films due to swelling have been quantified with profilometry⁵⁷ and scanning probe techniques,⁹⁰ and mass changes have been quantified with electrochemical quartz crystal microbalance (EQCM) methods.⁹¹ Electrolytes can swell OMIEC volume by several hundred percent.⁹² EQCM measurements have revealed that the compositional changes that accompany (de)doping of OMIECs are not as simple as those induced by dopant ion injection and expulsion. EQCM studies in both CP and radical polymer based OMIECs reveal a balance of dopant ion transport and oppositely charged

counter ion transport accompanied with neutral solvent incorporation that depends on the relative ion size, ion dissociation, and electrolyte concentration.^{93–95} The more massive the dopant ion, the more doping/de-doping occurs through counter ion transport.

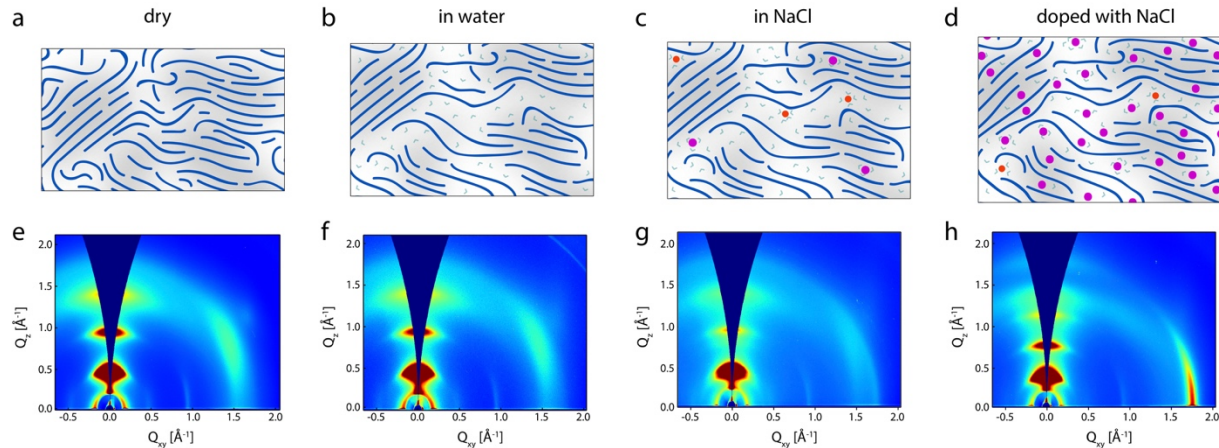


Figure 5. The profound influence of electrolyte on film structural characteristics. Cartoon schematics (a-d) of dry p(g2T-TT) (a), as well as swollen films exposed to water (b), exposed to aqueous electrolytes (c), and then biased at +0.5V vs Ag/AgCl (d). In a-d, blue denotes polymer chains with grey areas indicating crystallites, magenta denotes anions, orange denotes cations, and green denotes water (electronic charge on the polymer backbone not shown). Grazing incidence wide angle X-ray scattering plots (e-h) corresponding to the above conditions.⁸⁵ Dry films (e) show side-chain lamellar stacking out of plane and π -stacking in plane. Exposure to water (f) shows no changes and exposure to aqueous NaCl (g) disrupts lamellar and π -stacking showing a new scattering population. Ex situ electrochemical doping (h) drives ions into the crystallites expanding the lamellar stacking and contracts the π - π spacing shifting the out of plane scattering peaks to lower q values and in plane scattering peaks to higher q . Overall, doping increases the degree of π -stacking order manifest in increase scattering intensity, and narrowed peak widths. Note that no GIWAXS changes are observed when exposed to water, as the water does not affect crystallites, however, the films does swell >10%. Figure adapted from ref [85].

Structure-Property Relationships

With the goal of establishing structure property-relationships, OMIEC researchers have a wide array of characterization tools at their disposal. No single technique provides a structure-property panacea, however with a combination of device, scanning probe, scattering, and spectroscopic techniques OMIEC structure, mixed transport, and ionic-electronic coupling can be quantified and related across length scales (Fig. 6). To establish structure-property relations, structure characterization must be combined with methods for ionic transport, electronic transport, and ionic-electronic coupling determination. Since OMIECs are dynamic systems, relating structure and property at a single steady state or equilibrium condition is inadequate. Structure-property investigations must be carried out across a range of conditions, most often achieved by varying electrochemical potentials or electrolyte concentrations. Some examples of

studies that tackle these challenges are highlighted below, in lieu of a thorough recitation of all available techniques.

Ex-situ grazing incidence wide angle X-ray scattering (GIWAXS) (Fig. 6f) of type VI OMIECs has been combined with OECT studies to relate electronic charge transport to the crystalline modification that occurs upon water exposure, electrolyte exposure, and potential driven doping. This has revealed an evolution of crystalline microstructure that accompanies the ionic-electronic coupling (doping) that produces high conductivity in OMIECs (Fig. 5e-h).⁸⁵ Similar studies in CPs have shown these microstructural changes to be cumulative and irreversible under continuous device operation, with electrolyte swelling of amorphous domains randomizing crystallite orientation.⁹⁶ Studies of PEDOT:PSS combining GIWAXS and OECT studies with resonant soft X-ray scattering and moving front (Fig. 6c) ion transport techniques have revealed the development of a percolated microstructure advantageous for electronic transport leads to diminished ionic transport.⁹⁷

Similar studies in block OMIECs (type III & IV) have employed small angle scattering to correlate structure to ionic and electronic transport, revealing the long-range ordering of CP and polymer electrolyte blocks into lamellar structures.⁴⁰ This gives structural rationalization for the profound increase in ionic conductivity these block materials show over type II CPs/polymer electrolyte blends, showing the need for long range continuous pathways for efficient ionic transport.

While ex-situ structural studies have greatly advanced the understanding of OMIECs, they do not capture true device-relevant conditions. Crucial to understanding OMIEC structure-property relationships is understanding their electrolyte-swollen structure. Often, ex-situ samples are dried or undergo significant solvent loss before characterization. Further, ex-situ characterization cannot capture the dynamic structural transients that accompany OMIEC processes, thus operando and in-situ structural characterization are necessary. For example, operando wide angle scattering measurements of type IV battery materials with simultaneous

electronic transport measurements has precisely mapped the functional relationship between electronic mobility and CP block crystallite lattice strain.⁹⁸ Operando GIWAXS on CP-based OECTs combined with spectroscopic studies has confirmed this result and given evidence that though coupled, dopant ions preferentially reside in the disordered domains and electronic charge preferentially reside in the ordered domains.⁹⁹

This domain preference highlights the reality that many OMIECs have a significant amorphous fraction or are completely amorphous, and the information derived from X-ray scattering techniques is limited to the crystalline domains. Spectroscopic techniques present a possible operando or in-situ route to probe the amorphous domains. Recently Raman spectroscopy (Fig. 6e) has been used to probe the degree of ionic-electronic coupling in OMIECs.¹⁰⁰ Further, it has been employed as an in-situ measure of the degree and nature of electronic charging in CPs, with the ability to resolve differences in electronic charges based on whether it resides in ordered or disordered domains.¹⁰¹ In CP systems, a scanning probe technique called electrochemical strain microscopy,(Fig. 6d) has demonstrated the ability to both map the ordered/disordered heterogeneity and measure the domain-specific electrochemical potential dependent swelling and ion uptake. Such a technique has applicability for characterizing OMIECs used in thin film applications.¹⁰²

Parallel modelling of OMIEC systems can further exploit the structural information derived from the above techniques. Because OMIECs are complex systems with dynamic structure and mobile ions and solvent molecules, they present complex and computationally demanding systems to model. Molecular dynamics simulations have been reported that investigate the molecular scale structure and interactions and their effect on ionic and electronic transport, and ionic-electronic coupling.^{103–105} Further, multiscale modelling will be key to filling in the experimentally inaccessible gaps of structural and transport information.

The number of structure-property studies in OMIECs is still relatively limited, yet a clearer picture is starting to emerge. Ionic conductivity is synthetically achievable in homogenous

materials by making them ion-philic through ionic charge or ether oxygen-incorporating side chains, producing type V and VI OMIECs, respectively. Heterogenous OMIECs (type I-IV) that segregate the ionic and electronic transport phases often show better ionic transport, though at the expense of ionic-electronic coupling. Often the microstructure that improves electronic transport diminishes ionic transport and vice versa. Although the importance of these tradeoffs depends on the ultimate application of the OMIEC, there still remains much room for improvement of OMIEC materials which requires a better understanding of structure-property relationships.

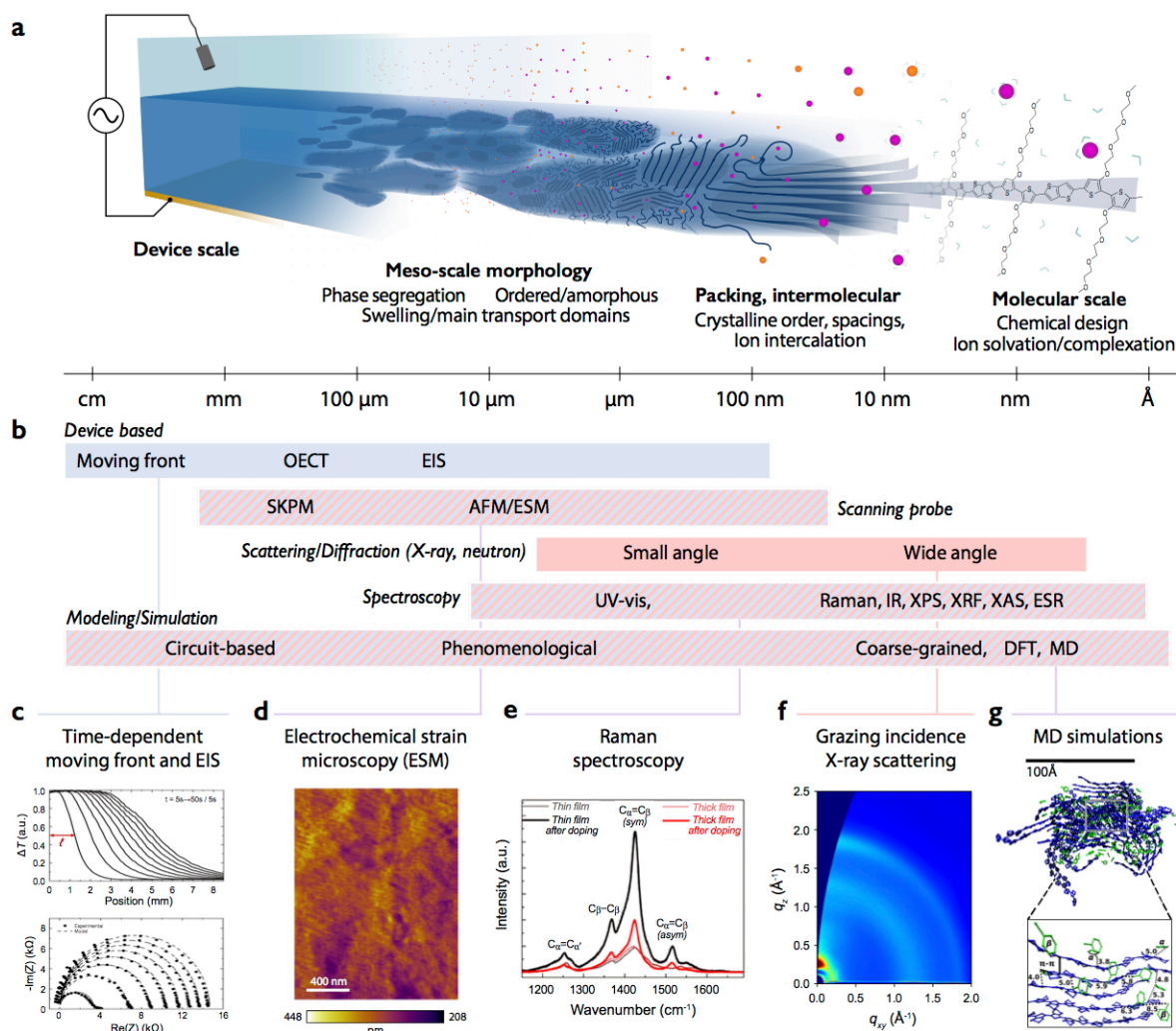


Figure 6. Multi-scale microstructure and associated techniques for studying OMIECs. (a) Device to molecular scale microstructure and interactions with an electrolyte. Magenta denotes anion, orange denotes cation. (b) Classes of characterization, and examples of specific techniques for probing transport and structure across these size scales. Blue denotes techniques that provide information about electronic/ionic transport and charging including organic electrochemical transistors (OECT), and electrochemical impedance spectroscopy (EIS). Pink denotes structural characterization. Many scanning probe and

spectroscopic techniques can provide detail associated with both structure and transport/charging, including scanning kelvin probe microscopy (SKPM), atomic force microscopy (AFM), electrochemical strain microscopy (ESM), ultraviolet and visible spectroscopy (UV-vis), Raman, infrared spectroscopy (IR), x-ray photoelectron spectroscopy (XPS), x-ray fluorescence (XRF), x-ray absorption spectroscopy (XAS), and electron spin resonance spectroscopy (ESR). Circuit based, phenomenological, coarse-grained, density function theory (DFT), and molecular dynamics (MD) modelling can give insight into both structure and transport. **c-g** highlight a selection of techniques that exemplify the different categories. **c)** Electrochromism⁵⁷ and impedance spectroscopy⁷⁷ on PEDOT:PSS moving front devices. **d)** Electrochemical strain microscopy measurements on P3HT gated in aqueous electrolyte.¹⁰² **e)** Raman spectroscopy on PEDOT:PSS films before and after electrochemical doping.¹⁰⁰ **f)** GIWAXS on PEDOT:PSS films. **g)** Molecular dynamics simulations on PEDOT:Tosylate including water (not shown).¹⁰³

Outlook

OMIECs represent an exciting, rising class of functional materials. They are especially attractive in a variety of applications due to their ability to efficiently store and transport both ionic and electronic charge and interconvert between the two. Further, the unique charge transport/storage properties of OMIECs enable sensing, light emitting, electrochromic, and actuating functionality, to name a few. OMIECs excel in these applications due to the complex interplay between the ionic charge solvated by or tethered to the OMIEC, and the electronic charge on the conjugated (macro)molecules. The dynamics of this ionic-electronic relationship drastically change over a wide range the OMIEC structure and externally applied potential. Producing robust structure-property relations for complex OMIEC systems remains an ongoing goal as these relationships are needed to guide materials design. Work remains to integrate characterization techniques into operando test beds to capture the dynamics of OMIEC systems. Coupling experimental results with rigorous modelling, both on the device and molecular scale, is key to clarifying the fundamental processes of OMIECs. Although reliable techniques exist for quantifying electronic transport and ionic-electronic coupling, ionic transport in OMIECs remains more difficult to assess. It is worth looking to the field of iontronic devices (ion pumps, diodes, transistors) for potential test beds for characterizing OMIEC ion transport.¹⁰⁶

The work ahead seems daunting, yet for the field of OMIECs this is a propitious moment. It is helpful to remember that in the broader field of organic electronics at the eve of this millennium, single junction organic solar cell efficiencies hovered at just barely 1% and carrier mobilities in organic field effect transistors only reached a few hundredths of a $\text{cm}^2 \text{V}^{-1} \text{s}^{-1}$. The important characterization work that clearly delineated organic semiconductor structure-

property relationships guided the purposeful synthetic, processing, and device design that led to single junction cells exceeding 10% PCE and OFETs with carrier mobility exceeding $10 \text{ cm}^2 \text{ V}^{-1} \text{ s}^{-1}$, with both technologies on the cusp of commercialization. Similar advances based on structural understanding in OMIECs are not improbable. The evidence of the power of establishing structure-property relations is all the more exciting for OMIECs due to their great promise across the fields of energy storage, chemical and biological sensing, medical devices, displays, light emission, printed circuits, and neuromorphic computing. However, this will only occur if rigorous fundamental structural in-situ/operando works across applications are carried out and broadly applied across the burgeoning field of organic mixed ionic electronic conductors.

Acknowledgements

B.P. and J.R. gratefully acknowledge support from the National Science Foundation Grant No. NSF DMR-1751308. K.T and E.S. gratefully acknowledge support from the Swedish Government Strategic Research Area in Materials Science on Advanced Functional Materials at Linköping University (Faculty Grant SFO-Mat-LiU No. 2009-00971). K.T. was also supported by the Swedish Foundation for Strategic Research and ES is supported by Vetenskapsrådet VR-2017-04910.

Competing financial interests

The authors declare no competing financial interests.

References

1. Elschner, A. *et al. PEDOT : Principles and Applications of an Intrinsically Conductive Polymer.* (CRC Press, 2010). doi:10.1201/b10318
2. Huang, F., Wu, H. & Cao, Y. Water /alcohol soluble conjugated polymers as highly efficient electron transporting/injection layer in optoelectronic devices. *Chem. Soc. Rev.* **39**, 2500–2521 (2010).
3. Snook, G. A., Kao, P. & Best, A. S. Conducting-polymer-based supercapacitor devices and electrodes. *J. Power Sources* **196**, 1–12 (2011).

4. Liang, Y., Tao, Z. & Chen, J. Organic Electrode Materials for Rechargeable Lithium Batteries. *Adv. Energy Mater.* **2**, 742–769 (2012).
5. Smela, E. Conjugated Polymer Actuators for Biomedical Applications. *Adv. Mater.* **15**, 481–494 (2003).
6. Pei, Q., Yu, G., Zhang, C., Yang, Y. & Heeger, A. J. Polymer Light-Emitting Electrochemical Cells. *Science* **269**, 1086–1088 (1995).
7. Jang, J., Ha, J. & Cho, J. Fabrication of Water-Dispersible Polyaniline-Poly(4-styrenesulfonate) Nanoparticles For Inkjet-Printed Chemical-Sensor Applications. *Adv. Mater.* **19**, 1772–1775 (2007).
8. Ludwig, K. A., Uram, J. D., Yang, J., Martin, D. C. & Kipke, D. R. Chronic neural recordings using silicon microelectrode arrays electrochemically deposited with a poly(3,4-ethylenedioxythiophene) (PEDOT) film. *J. Neural Eng.* **3**, 59 (2006).
9. Isaksson, J. *et al.* Electronic control of Ca^{2+} signalling in neuronal cells using an organic electronic ion pump. *Nat. Mater.* **6**, 673–679 (2007).
10. Rivnay, J. *et al.* Organic electrochemical transistors. *Nat. Rev. Mater.* **3**, 17086 (2018).
11. Burgt, Y. van de *et al.* A non-volatile organic electrochemical device as a low-voltage artificial synapse for neuromorphic computing. *Nat. Mater.* **16**, 414–418 (2017).
12. Sunarso, J. *et al.* Mixed ionic–electronic conducting (MIEC) ceramic-based membranes for oxygen separation. *J. Membr. Sci.* **320**, 13–41 (2008).
13. Chueh, W. C. & Haile, S. M. Electrochemistry of Mixed Oxygen Ion and Electron Conducting Electrodes in Solid Electrolyte Cells. *Annu. Rev. Chem. Biomol. Eng.* **3**, 313–341 (2012).
14. Li, W., Liu, J. & Zhao, D. Mesoporous materials for energy conversion and storage devices. *Nat. Rev. Mater.* **1**, (2016).
15. Liu, Y., Duzhko, V. V., Page, Z. A., Emrick, T. & Russell, T. P. Conjugated Polymer Zwitterions: Efficient Interlayer Materials in Organic Electronics. *Acc. Chem. Res.* **49**, 2478–2488 (2016).
16. Stavrinidou, E. *et al.* Engineering hydrophilic conducting composites with enhanced ion mobility. *Phys. Chem. Chem. Phys.* **16**, 2275–2279 (2014).
17. Harman, D. G. *et al.* Poly(3,4-ethylenedioxythiophene):dextran sulfate (PEDOT:DS) – A highly processable conductive organic biopolymer. *Acta Biomater.* **14**, 33–42 (2015).
18. Cui, X., Hetke, J. F., Wiler, J. A., Anderson, D. J. & Martin, D. C. Electrochemical deposition and characterization of conducting polymer polypyrrole/PSS on multichannel neural probes. *Sens. Actuators Phys.* **93**, 8–18 (2001).
19. Cao, Y., Yu, G., Heeger, A. J. & Yang, C. Y. Efficient, fast response light-emitting electrochemical cells: Electroluminescent and solid electrolyte polymers with interpenetrating network morphology. *Appl. Phys. Lett.* **68**, 3218–3220 (1996).
20. Moon, H. C. & Kim, J. K. Phase segregation of poly(3-dodecylthiophene)-block-poly(methyl methacrylate) copolymers. *Polymer* **54**, 5437–5442 (2013).

21. Gu, Z., Kanto, T., Tsuchiya, K. & Ogino, K. Synthesis of Poly(3-hexylthiophene)-b-poly(ethylene oxide) for Application to Photovoltaic Device. *J. Photopolym. Sci. Technol.* **23**, 405–406 (2010).
22. Kato, T. *et al.* Transport of ions and electrons in nanostructured liquid crystals. *Nat. Rev. Mater.* **2**, 17001 (2017).
23. Patel, S. N. *et al.* Morphology and Thermodynamic Properties of a Copolymer with an Electronically Conducting Block: Poly(3-ethylhexylthiophene)-block-poly(ethylene oxide). *Nano Lett.* **12**, 4901–4906 (2012).
24. Erothu, H. *et al.* Synthesis, Thermal Processing, and Thin Film Morphology of Poly(3-hexylthiophene)–Poly(styrenesulfonate) Block Copolymers. *Macromolecules* **48**, 2107–2117 (2015).
25. Gutacker, A. *et al.* All-conjugated polyelectrolyte block copolymers. *J. Mater. Chem.* **20**, 1423–1430 (2010).
26. Chen, X., Zhang, Z., Ding, Z., Liu, J. & Wang, L. Diketopyrrolopyrrole-based Conjugated Polymers Bearing Branched Oligo(Ethylene Glycol) Side Chains for Photovoltaic Devices. *Angew. Chem.* **128**, 10532–10536 (2016).
27. Brendel, J. C., Schmidt, M. M., Hagen, G., Moos, R. & Thelakkat, M. Controlled Synthesis of Water-Soluble Conjugated Polyelectrolytes Leading to Excellent Hole Transport Mobility. *Chem. Mater.* **26**, 1992–1998 (2014).
28. Inal, S. *et al.* A High Transconductance Accumulation Mode Electrochemical Transistor. *Adv. Mater.* **26**, 7450–7455 (2014).
29. Karlsson, R. H. *et al.* Iron-Catalyzed Polymerization of Alkoxysulfonate-Functionalized 3,4-Ethylenedioxythiophene Gives Water-Soluble Poly(3,4-ethylenedioxythiophene) of High Conductivity. *Chem. Mater.* **21**, 1815–1821 (2009).
30. Jiang, H., Taranekar, P., Reynolds, J. R. & Schanze, K. S. Conjugated Polyelectrolytes: Synthesis, Photophysics, and Applications. *Angew. Chem. Int. Ed.* **48**, 4300–4316 (2009).
31. Liu, B. & Bazan, G. C. *Conjugated Polyelectrolytes: Fundamentals and Applications*. (John Wiley & Sons, 2013).
32. Nielsen, C. B. *et al.* Molecular Design of Semiconducting Polymers for High-Performance Organic Electrochemical Transistors. *J. Am. Chem. Soc.* **138**, 10252–10259 (2016).
33. Giovannitti, A. *et al.* N-type organic electrochemical transistors with stability in water. *Nat. Commun.* **7**, 13066 (2016).
34. Savagian, L. R. *et al.* Balancing Charge Storage and Mobility in an Oligo(Ether) Functionalized Dioxythiophene Copolymer for Organic- and Aqueous- Based Electrochemical Devices and Transistors. *Adv. Mater.* **30**, 1804647 (2018).
35. Giovannitti, A. *et al.* Controlling the mode of operation of organic transistors through side-chain engineering. *Proc. Natl. Acad. Sci.* **113**, 12017–12022 (2016).

36. Slinker, J.D. *et al.* Electroluminescent devices from ionic transition metal complexes. *J. Mater. Chem.* **17**, 2976–2988 (2007).
37. Janoschka, T., Hager, M. D. & Schubert, U. S. Powering up the Future: Radical Polymers for Battery Applications. *Adv. Mater.* **24**, 6397–6409 (2012).
38. Moia, D. *et al.* Design and evaluation of conjugated polymers with polar side chains as electrode materials for electrochemical energy storage in aqueous electrolytes. *Energy Environ. Sci.* **12**, 1349–1357 (2019).
39. Javier, A. E., Patel, S. N., Hallinan, D. T., Srinivasan, V. & Balsara, N. P. Simultaneous Electronic and Ionic Conduction in a Block Copolymer: Application in Lithium Battery Electrodes. *Angew. Chem. Int. Ed.* **50**, 9848–9851 (2011).
40. Patel, S. N., Javier, A. E., Stone, G. M., Mullin, S. A. & Balsara, N. P. Simultaneous Conduction of Electronic Charge and Lithium Ions in Block Copolymers. *ACS Nano* **6**, 1589–1600 (2012).
41. Winther-Jensen, B., Winther-Jensen, O., Forsyth, M. & MacFarlane, D. R. High Rates of Oxygen Reduction over a Vapor Phase–Polymerized PEDOT Electrode. *Science* **321**, 671–674 (2008).
42. Rudolph, M. & Ratcliff, E. L. Normal and inverted regimes of charge transfer controlled by density of states at polymer electrodes. *Nat. Commun.* **8**, 1048 (2017).
43. Mitraka, E. *et al.* Electrocatalytic Production of Hydrogen Peroxide with Poly(3,4-ethylenedioxythiophene) Electrodes. *Adv. Sustain. Syst.* **3**, 1800110 (2019).
44. Inal, S., Malliaras, G. G. & Rivnay, J. Benchmarking organic mixed conductors for transistors. *Nat. Commun.* **8**, 1767 (2017).
45. Noriega, R. *et al.* A general relationship between disorder, aggregation and charge transport in conjugated polymers. *Nat. Mater.* **12**, 1038–1044 (2013).
46. Tessler, N., Preezant, Y., Rappaport, N. & Roichman, Y. Charge Transport in Disordered Organic Materials and Its Relevance to Thin-Film Devices: A Tutorial Review. *Adv. Mater.* **21**, 2741–2761 (2009).
47. Coropceanu, V. *et al.* Charge Transport in Organic Semiconductors. *Chem. Rev.* **107**, 926–952 (2007).
48. Kunugi, Y., Harima, Y., Yamashita, K., Ohta, N. & Ito, S. Charge transport in a regioregular poly(3-octylthiophene) film. *J. Mater. Chem.* **10**, 2673–2677 (2000).
49. Wang, S., Ha, M., Manno, M., Daniel Frisbie, C. & Leighton, C. Hopping transport and the Hall effect near the insulator–metal transition in electrochemically gated poly(3-hexylthiophene) transistors. *Nat. Commun.* **3**, 1210 (2012).
50. Paulsen, B. D. & Frisbie, C. D. Dependence of Conductivity on Charge Density and Electrochemical Potential in Polymer Semiconductors Gated with Ionic Liquids. *J. Phys. Chem. C* **116**, 3132–3141 (2012).

51. Sato, K. *et al.* Diffusion-Cooperative Model for Charge Transport by Redox-Active Nonconjugated Polymers. *J. Am. Chem. Soc.* **140**, 1049–1056 (2018).
52. Kemper, T. W., Larsen, R. E. & Gennett, T. Density of States and the Role of Energetic Disorder in Charge Transport in an Organic Radical Polymer in the Solid State. *J. Phys. Chem. C* **119**, 21369–21375 (2015).
53. Joo, Y., Agarkar, V., Sung, S. H., Savoie, B. M. & Boudouris, B. W. A nonconjugated radical polymer glass with high electrical conductivity. *Science* **359**, 1391–1395 (2018).
54. Collins, S. D. *et al.* Observing Ion Motion in Conjugated Polyelectrolytes with Kelvin Probe Force Microscopy. *Adv. Electron. Mater.* **3**, 1700005 (2017).
55. Reenen, S. van, Janssen, R. A. J. & Kemerink, M. Dynamic Processes in Sandwich Polymer Light-Emitting Electrochemical Cells. *Adv. Funct. Mater.* **22**, 4547–4556 (2012).
56. Merkle, R. *et al.* Mixed conductivity of polythiophene-based ionic polymers under controlled conditions. *Polymer* **132**, 216–226 (2017).
57. Stavrinidou, E. *et al.* Direct Measurement of Ion Mobility in a Conducting Polymer. *Adv. Mater.* **25**, 4488–4493 (2013).
58. Amdursky, N., Głowacki, E. D. & Meredith, P. Macroscale Biomolecular Electronics and Ionics. *Adv. Mater.* **31**, 1802221 (2019).
59. Park, M., Zhang, X., Chung, M., Less, G. B. & Sastry, A. M. A review of conduction phenomena in Li-ion batteries. *J. Power Sources* **195**, 7904–7929 (2010).
60. Lai, W. & Haile, S. M. Impedance Spectroscopy as a Tool for Chemical and Electrochemical Analysis of Mixed Conductors: A Case Study of Ceria. *J. Am. Ceram. Soc.* **88**, 2979–2997 (2005).
61. Barsoukov, E. & Macdonald, J. R. *Impedance Spectroscopy: Theory, Experiment, and Applications*. (John Wiley & Sons, 2018).
62. Garcia-Belmonte, G., Bisquert, J. & Popkirov, G. S. Determination of the electronic conductivity of polybithiophene films at different doping levels using in situ electrochemical impedance measurements. *Appl. Phys. Lett.* **83**, 2178–2180 (2003).
63. Ren, X. & Pickup, P. G. Ion transport in polypyrrole and a polypyrrole/polyanion composite. *J. Phys. Chem.* **97**, 5356–5362 (1993).
64. Sheliakina, M., Mostert, A. B. & Meredith, P. Decoupling Ionic and Electronic Currents in Melanin. *Adv. Funct. Mater.* **28**, 1805514 (2018).
65. Bisquert, J. *et al.* A review of recent results on electrochemical determination of the density of electronic states of nanostructured metal-oxide semiconductors and organic hole conductors. *Inorganica Chim. Acta* **361**, 684–698 (2008).
66. Bisquert, J., Garcia-Belmonte, G. & Pitarch, Á. An Explanation of Anomalous Diffusion Patterns Observed in Electroactive Materials by Impedance Methods. *ChemPhysChem* **4**, 287–292 (2003).

67. Jamnik, J. & Maier, J. Treatment of the Impedance of Mixed Conductors Equivalent Circuit Model and Explicit Approximate Solutions. *J. Electrochem. Soc.* **146**, 4183–4188 (1999).

68. Bernards, D. A. & Malliaras, G. G. Steady-State and Transient Behavior of Organic Electrochemical Transistors. *Adv. Funct. Mater.* **17**, 3538–3544 (2007).

69. Rivnay, J. *et al.* Organic electrochemical transistors for cell-based impedance sensing. *Appl. Phys. Lett.* **106**, 043301 (2015).

70. Trefz, D. *et al.* Electrochemical Investigations of the N-Type Semiconducting Polymer P(NDI2OD-T2) and Its Monomer: New Insights in the Reduction Behavior. *J. Phys. Chem. C* **119**, 22760–22771 (2015).

71. Kaake, L. G. & Zhu, X.-Y. Charge Transport, Nanostructure, and the Mott Insulator-to-Metal Transition in Poly(3-hexylthiophene). *J. Phys. Chem. C* **112**, 16174–16177 (2008).

72. Mostert, A. B. *et al.* Role of semiconductivity and ion transport in the electrical conduction of melanin. *Proc. Natl. Acad. Sci.* **109**, 8943–8947 (2012).

73. Tezuka, Y., Ohyama, S., Ishii, T. & Aoki, K. Observation of Propagation Speed of Conductive Front in Electrochemical Doping Process of Polypyrrole Films. *Bull. Chem. Soc. Jpn.* **64**, 2045–2051 (1991).

74. Aoki, K., Aramoto, T. & Hoshino, Y. Photographic measurements of propagation speeds of the conducting zone in polyaniline films during electrochemical switching. *J. Electroanal. Chem.* **340**, 127–135 (1992).

75. Carlberg, J. C. & Inganäs, O. Fast Optical Spectroscopy of the Electrochemical Doping of Poly(3,4-ethylenedioxythiophene). *J. Electrochem. Soc.* **145**, 3810–3814 (1998).

76. Wang, X. & Smela, E. Experimental Studies of Ion Transport in PPy(DBS). *J. Phys. Chem. C* **113**, 369–381 (2009).

77. Stavrinidou, E., Sessolo, M., Winther-Jensen, B., Sanaur, S. & Malliaras, G. G. A physical interpretation of impedance at conducting polymer/electrolyte junctions. *AIP Adv.* **4**, 017127 (2014).

78. Feldberg, S. W. Reinterpretation of polypyrrole electrochemistry. Consideration of capacitive currents in redox switching of conducting polymers. *J. Am. Chem. Soc.* **106**, 4671–4674 (1984).

79. Yeu, T., Nguyen, T. V. & White, R. E. A Mathematical Model for Predicting Cyclic Voltammograms of Electronically Conductive Polypyrrole. *J. Electrochem. Soc.* **135**, 1971–1976 (1988).

80. Friedlein, J. T. *et al.* Influence of disorder on transfer characteristics of organic electrochemical transistors. *Appl. Phys. Lett.* **111**, 023301 (2017).

81. Tybrandt, K., Zozoulenko, I. V. & Berggren, M. Chemical potential–electric double layer coupling in conjugated polymer–polyelectrolyte blends. *Sci. Adv.* **3**, eaao3659 (2017).

82. Facchetti, A. π -Conjugated Polymers for Organic Electronics and Photovoltaic Cell Applications. *Chem. Mater.* **23**, 733–758 (2011).

83. Zhang, H. & Shen, P. K. Recent Development of Polymer Electrolyte Membranes for Fuel Cells. *Chem. Rev.* **112**, 2780–2832 (2012).

84. Ratner, M. A. & Shriver, D. F. Ion transport in solvent-free polymers. *Chem. Rev.* **88**, 109–124 (1988).

85. Cendra, C. *et al.* Role of the Anion on the Transport and Structure of Organic Mixed Conductors. *Adv. Funct. Mater.* **29**, 1807034 (2019).

86. Slinker, J. D. *et al.* Direct measurement of the electric-field distribution in a light-emitting electrochemical cell. *Nat. Mater.* **6**, 894–899 (2007).

87. Matyba, P., Maturova, K., Kemerink, M., Robinson, N. D. & Edman, L. The dynamic organic p–n junction. *Nat. Mater.* **8**, 672–676 (2009).

88. Francis, C. *et al.* Raman Spectroscopy and Microscopy of Electrochemically and Chemically Doped High-mobility Semiconducting Polymers. *J. Mater. Chem. C.* **5**, 6176–6184 (2017).

89. Wada, Y., Enokida, I., Yamamoto, J. & Furukawa, Y. Raman imaging of carrier distribution in the channel of an ionic liquid-gated transistor fabricated with regioregular poly(3-hexylthiophene). *Spectrochim. Acta. A. Mol. Biomol. Spectrosc.* **197**, 166–169 (2018).

90. Smela, E. & Gadegaard, N. Surprising Volume Change in PPy(DBS): An Atomic Force Microscopy Study. *Adv. Mater.* **11**, 953–957 (1999).

91. Flagg, L. Q. *et al.* Polymer Crystallinity Controls Water Uptake in Glycol Side-Chain Polymer Organic Electrochemical Transistors. *J. Am. Chem. Soc.* **141**, 4345–4354 (2019).

92. ElMahmoudy, M. *et al.* Tailoring the Electrochemical and Mechanical Properties of PEDOT:PSS Films for Bioelectronics. *Macromol. Mater. Eng.* **302**, 1600497 (2017).

93. Naoi, K., Lien, M. & Smyrl, W. H. Quartz Crystal Microbalance Study: Ionic Motion Across Conducting Polymers. *J. Electrochem. Soc.* **138**, 440–445 (1991).

94. Qiu, Y.-J. & Reynolds, J. R. Dopant anion controlled ion transport behavior of polypyrrole. *Polym. Eng. Sci.* **31**, 417–421 (1991).

95. Wang, S., Li, F., Easley, A. D. & Lutkenhaus, J. L. Real-time insight into the doping mechanism of redox-active organic radical polymers. *Nat. Mater.* **18**, 69–75 (2019).

96. Guardado, J. O. & Salleo, A. Structural Effects of Gating Poly(3-hexylthiophene) through an Ionic Liquid. *Adv. Funct. Mater.* **27**, 1701791 (2017).

97. Rivnay, J. *et al.* Structural control of mixed ionic and electronic transport in conducting polymers. *Nat. Commun.* **7**, 11287 (2016).

98. Thelen, J. L. *et al.* Relationship between Mobility and Lattice Strain in Electrochemically Doped Poly(3-hexylthiophene). *ACS Macro Lett.* **4**, 1386–1391 (2015).

99. Thomas, E. M. *et al.* X-Ray Scattering Reveals Ion-Induced Microstructural Changes During Electrochemical Gating of Poly(3-Hexylthiophene). *Adv. Funct. Mater.* **28**, 1803687 (2018).

100. Savva, A., Wustoni, S. & Inal, S. Ionic-to-electronic coupling efficiency in PEDOT:PSS films operated in aqueous electrolytes. *J. Mater. Chem. C* **6**, 12023–12030 (2018).

101. Nightingale, J., Wade, J., Moia, D., Nelson, J. & Kim, J.-S. Impact of Molecular Order on Polaron Formation in Conjugated Polymers. *J. Phys. Chem. C* **122**, 29129–29140 (2018).
102. Giridharagopal, R. *et al.* Electrochemical strain microscopy probes morphology-induced variations in ion uptake and performance in organic electrochemical transistors. *Nat. Mater.* **16**, 737–742 (2017).
103. Franco-Gonzalez, J. F. & Zozoulenko, I. V. Molecular Dynamics Study of Morphology of Doped PEDOT: From Solution to Dry Phase. *J. Phys. Chem. B* **121**, 4299–4307 (2017).
104. Modarresi, M., Felipe Franco-Gonzalez, J. & Zozoulenko, I. Morphology and ion diffusion in PEDOT:Tos. A coarse grained molecular dynamics simulation. *Phys. Chem. Chem. Phys.* **20**, 17188–17198 (2018).
105. Dong, B. X. *et al.* Influence of Side-Chain Chemistry on Structure and Ionic Conduction Characteristics of Polythiophene Derivatives: A Computational and Experimental Study. *Chem. Mater.* **31**, 1418–1429 (2019).
106. Sjöström, T. A. *et al.* A Decade of Iontronic Delivery Devices. *Adv. Mater. Technol.* **3**, 1700360 (2018).
107. van Reenen, S., Akatsuka, T., Tordera, D., Kemerink, M. & Bolink, H. J. Universal Transients in Polymer and Ionic Transition Metal Complex Light-Emitting Electrochemical Cells. *J. Am. Chem. Soc.* **135**, 886–891 (2013).
108. Renna, L. A., Lenef, J. D., Bag, M. & Venkataraman, D. Mixed Ionic–Electronic Conduction in Binary Polymer Nanoparticle Assemblies. *Adv. Mater. Interfaces* **4**, 1700397 (2017).
109. McNaught, A. D., Wilkinson, A., Jenkins, A. D. & International Union of Pure and Applied Chemistry. *IUPAC compendium of chemical terminology : the gold book.* (International Union of Pure and Applied Chemistry, 2006).
110. Berggren, M. & Malliaras, G. G. How conducting polymer electrodes operate. *Science* **364**, 233–234 (2019).